

# Bright-White Light-Emitting Devices Based on a Single Polymer Exhibiting Simultaneous Blue, Green, and Red Emissions

Chu-Ying Chuang, Ping-I Shih, Chen-Han Chien, Fang-Iy Wu, and Ching-Fong Shu\*

Department of Applied Chemistry, National Chiao Tung University, 300 Hsinchu, Taiwan

Received September 21, 2006; Revised Manuscript Received November 9, 2006

**ABSTRACT:** We have developed efficient white-light-emitting polymers through the incorporation of low band gap green-light-emitting benzothiadiazole and red-light-emitting bithiophenylbenzothiadiazole moieties into the backbone of a blue-light-emitting bipolar polyfluorene copolymer. Partial energy transfer from the blue-fluorescent polyfluorene backbone to the green- and red-fluorescent components resulted in individual emissions from the three emissive species. By carefully controlling the concentrations of the low-energy-emitting species in the resulting copolymers, the emission of white light, with contributions from each of the three primary colors, was achieved. Efficient polymer light-emitting devices prepared using these copolymers exhibited luminance efficiencies as high as 4.87 cd/A with color coordinates (0.37, 0.36) that were very close to the ideal CIE chromaticity coordinates for pure white light (0.33, 0.33). In addition, the color coordinates remained almost unchanged over a range of operating potentials. A mechanistic study suggested that energy transfer from the fluorene segments to the low band gap units, rather than charge trapping, was the main operating process involved in the electroluminescent process.

## Introduction

White organic light-emitting diodes (WOLEDs) have received considerable attention because of their potential for application in solid-state lighting and in backplane lighting for liquid crystal displays.<sup>1</sup> Among these devices, white-light OLEDs based on semiconductor polymers (PLEDs) are of particular interest for their ready solution-processibility, which allows spin-coating and printing methods to be utilized for the preparation of large-area-display devices.<sup>2</sup> In principle, the emission color of polymers can be easily tuned through covalently binding a guest chromophore to an emissive polymeric host at appropriate doping levels, which typically results in the partial or complete quenching of the host emission and the emergence of the dye emission. By tuning the dye concentration to realize complete energy transfer, devices exhibiting improved efficiencies and saturated red, green, and blue (RGB) colors have been realized.<sup>3</sup> Polyfluorenes (PFs) that emit in the blue region are very promising candidates for light-emitting materials because of their high photoluminescence (PL) and electroluminescence (EL) efficiencies and high thermal stabilities.<sup>4</sup> In addition, PFs can be readily color-tuned through chemical incorporation of low band gap comonomers or through physically doping with lower-energy fluorescent and phosphorescent dyes.<sup>5,6</sup> Consequently, PFs can function as both the host and the blue emitter in white-light-emitting devices. Several authors have reported white emissions from dye-functionalized PF copolymers.<sup>7</sup> For example, Tu et al.<sup>7b</sup> demonstrated that dichromatic white light could be achieved from a polyfluorene copolymer chemically doped with 1,8-naphthalimide segments at a very low concentration. In this case, the combination of a blue emission from the fluorene segments and an orange emission from the 1,8-naphthalimide segments led to the human visual perception of emitted white light. Recently, Liu et al.<sup>7c</sup> successfully achieved a white electroluminescence (EL) comprising the three primary colors based on a PF copolymer prepared through Suzuki copolymerization with a small amount of a fluorescent green

chromophore attached to the side chain and a red chromophore covalently bound to the polymer backbone. This device exhibited a maximum brightness of 3786 cd/m<sup>2</sup> at 19.4 V and a maximum luminance efficiency of 1.59 cd/A.

We have demonstrated that **PFTO**, a bipolar charge-transporting polyfluorene derivative, is not merely an efficient blue emitter but also an ideal polymeric host for low-energy dopants.<sup>8</sup> In this study, therefore, we incorporated red and green fluorescent components into this bipolar PF copolymer with the aim of achieving white light emission from a single PF copolymer. The green- and red-emitting moieties in these copolymers were formed by incorporating small amounts of 4,7-dibromo-2,1,3-benzothiadiazole (**3**)<sup>5a</sup> and 4,7-bis(5-bromothiophen-2-yl)-2,1,3-benzothiadiazole (**4**),<sup>5b</sup> respectively, in the copolymerization mixture. By carefully controlling the concentrations of these low-energy-emitting species in the resulting copolymers, white electroluminescence, with contributions from all three primary colors, was achieved, accompanied by a maximum luminance efficiency of 4.87 cd/A, which corresponds to an external quantum efficiency of 2.22%.

## Experimental Section

**Materials.** Monomers **1–5** and copolymer **PFTO** were prepared according to reported procedures.<sup>5a,b,8a,9</sup> The solvents were dried using standard procedures. All other reagents were used as received from commercial sources unless otherwise stated.

**Characterization.** <sup>1</sup>H and <sup>13</sup>C NMR spectra were recorded on Varian UNITY INOVA AS500 (500 MHz) and Bruker-DRX 300 (300 MHz) spectrometers. Mass spectra were obtained using a JEOL JMS-HX 110 mass spectrometer. Size exclusion chromatography (SEC) was performed using a Waters chromatography unit interfaced with a Waters 410 differential refractometer; three 5 μm Waters styragel columns (300 mm × 7.8 mm) were connected in series in order of decreasing pore size (10<sup>4</sup>, 10<sup>3</sup>, and 10<sup>2</sup> Å); THF was the eluent. Standard polystyrene samples were used for calibration. Differential scanning calorimetry (DSC) was performed using a SEIKO EXSTAR 6000DSC unit at heating and cooling rates of 20 and 40 °C min<sup>-1</sup>, respectively. Samples were scanned from 30 to 250 °C, cooled to 0 °C, and then scanned again from 30 to 250 °C. The glass transition temperatures (*T*<sub>g</sub>) were determined

\* Corresponding author. E-mail: shu@cc.nctu.edu.tw.

from the second heating scan. Thermogravimetric analysis (TGA) was undertaken using a DuPont TGA 2950 instrument. The thermal stabilities of the samples were determined under a nitrogen atmosphere by measuring their weight loss while heating at a rate of 20 °C min<sup>-1</sup>. UV-vis spectra were measured using an HP 8453 diode-array spectrophotometer. PL spectra were obtained from a Hitachi F-4500 luminescence spectrometer. The ionization potentials of organic thin films were measured using a Riken-Keiki AC-2 atmospheric low-energy photoelectron spectrometer.<sup>10</sup>

**Fabrication of Light-Emitting Devices.** LED devices were fabricated in the form ITO/poly(styrenesulfonate)-doped poly(3,4-ethylenedioxythiophene) (PEDOT) (35 nm)/polymer emitting layer (50–70 nm)/TPBI (30 nm)/Mg:Ag (100 nm)/Ag(100 nm). The PEDOT was spin-coated directly onto the ITO glass and dried at 80 °C for 12 h under vacuum to improve the hole injection capability and increase the substrate's smoothness. The light-emitting layer was spin-coated on top of the PEDOT layer using chlorobenzene as the solvent; the sample was then dried for 3 h at 60 °C under vacuum. Prior to film casting, the polymer solution was filtered through a Teflon filter (0.45 μm). The TPBI layer, which was used as an electron-transporting layer that would also block holes and confine excitons, was grown through thermal sublimation in a vacuum (3 × 10<sup>-6</sup> Torr).<sup>11</sup> Subsequently, the cathode Mg:Ag (10:1, 100 nm) alloy was deposited through coevaporation onto the TPBI layer; this process was followed by placing an additional layer of Ag (100 nm) onto the alloy as a protection layer. The current-voltage-luminance relationships were measured under ambient conditions using a Keithley 2400 source meter and a Newport 1835C optical meter equipped with an 818ST silicon photodiode.

**4,7-Bis(9,9-dihexylfluoren-2-yl)-2,1,3-benzothiadiazole (GM).** A mixture of 4,7-dibromo-2,1,3-benzothiadiazole (**3**, 90.0 mg, 306 μmol), 2-(9,9-dihexylfluoren-7-yl)-4,4,5,5-tetramethyl-1,3,2-dioxaborolane<sup>12</sup> (330 mg, 717 μmol), Aliquat 336 (ca. 9 mg), aqueous K<sub>2</sub>CO<sub>3</sub> (2.0 M, 2.0 mL), and toluene (10 mL) was degassed; tetrakis(triphenylphosphine)palladium (ca. 8 mg) was then added while flushing vigorously with nitrogen. After heating at 105 °C for 12 h, the reaction mixture was poured into water (10 mL) and extracted with EtOAc (2 × 10 mL). The organic extracts were dried (MgSO<sub>4</sub>) and concentrated under reduced pressure. The residue was purified through column chromatography (CH<sub>2</sub>Cl<sub>2</sub>/*n*-hexane, 1:4) to afford **GM** (156 mg, 63.7%). <sup>1</sup>H NMR (300 MHz, CDCl<sub>3</sub>): δ 0.62–0.76 (m, 20H), 1.02–1.09 (m, 24H), 1.88–2.03 (m, 8H), 7.23–7.33 (m, 6H), 7.70 (dd, *J* = 5.9, 1.7 Hz, 2H), 7.79 (d, *J* = 8.4 Hz, 2H), 7.81 (s, 2H), 7.88 (d, *J* = 0.9 Hz, 2H), 7.94 (dd, *J* = 8.0, 1.7 Hz, 2H). <sup>13</sup>C NMR (75 MHz, CDCl<sub>3</sub>): δ 14.0, 22.6, 23.8, 29.7, 31.5, 40.3, 55.2, 119.7, 120.0, 122.9, 123.9, 126.8, 127.2, 127.9, 128.1, 133.6, 136.2, 140.7, 141.3, 151.1, 151.3, 154.4. HRMS (*m/z*): [M<sup>+</sup>] calcd for C<sub>56</sub>H<sub>68</sub>N<sub>2</sub>S, 800.5103; found, 800.5109.

**4,7-Bis[5-(9,9-dihexylfluoren-2-yl)thiophen-2-yl]-2,1,3-benzothiadiazole (RM).** Using the procedure described for **GM**, the Suzuki coupling reaction between 4,7-bis(5-bromothiophen-2-yl)-2,1,3-benzothiadiazole (**4**, 100 mg, 218 μmol) and 2-(9,9-dihexylfluoren-7-yl)-4,4,5,5-tetramethyl-1,3,2-dioxaborolane (221 mg, 480 μmol), followed by column chromatography (EtOAc/*n*-hexane, 1:10) and recrystallization from *n*-hexane, gave **RM** (84.9 mg, 40.4%). <sup>1</sup>H NMR (300 MHz, CDCl<sub>3</sub>): δ 0.64–0.66 (m, 8H), 0.74 (t, *J* = 6.8 Hz, 12H), 1.05–1.13 (m, 24H), 1.98–2.04 (m, 8H), 7.29–7.35 (m, 6H), 7.48 (d, *J* = 3.9 Hz, 2H), 7.65 (s, 2H), 7.70 (m, 6H), 7.93 (s, 2H), 8.14 (d, *J* = 3.9 Hz, 2H). <sup>13</sup>C NMR (75 MHz, CDCl<sub>3</sub>): δ 14.0, 22.6, 23.7, 29.7, 31.5, 40.4, 55.2, 119.8, 120.0, 120.1, 122.9, 123.9, 124.7, 125.3, 125.7, 126.8, 127.2, 128.6, 132.8, 138.3, 140.5, 141.1, 146.5, 150.9, 151.6, 152.6. HRMS (*m/z*): [M<sup>+</sup> + H] calcd for C<sub>64</sub>H<sub>73</sub>N<sub>2</sub>S<sub>3</sub>, 965.4936; found, 965.4943.

**Preparation of WPFTO-II.** Aqueous K<sub>2</sub>CO<sub>3</sub> (2.0 M, 2.0 mL) was added under a nitrogen atmosphere to a mixture of monomers **1** (47.3 mg, 53.9 μmol), **2** (55.5 mg, 53.6 μmol), **3** (6.80 × 10<sup>-3</sup> M in toluene, 128 μL, 0.87 μmol), **4** (1.09 × 10<sup>-3</sup> M in toluene, 440 μL, 0.48 μmol), **5** (70.0 mg, 109 μmol), and Aliquat 336 (ca. 13 mg) in toluene (1.5 mL). Tetrakis(triphenylphosphine)palladium (ca. 2 mg) was added while flushing vigorously with nitrogen, and

then the mixture was heated at 105 °C for 36 h. The end groups were capped by heating the resulting mixture under reflux for 8 h with benzenboronic acid (26.6 mg, 220 μmol) and then for 8 h with bromobenzene (34 mg, 220 μmol). The mixture was cooled to room temperature and the product precipitated into a mixture of MeOH and H<sub>2</sub>O (7:3) to obtain the crude polymer, which was dissolved in THF, reprecipitated into MeOH, and then washed with acetone for 48 h using a Soxhlet apparatus. Drying under vacuum gave **WPFTO-II** (95.9 mg, 74.4%). <sup>1</sup>H NMR (300 MHz, CDCl<sub>3</sub>): δ 0.68–0.74 (m, 20H), 0.86–0.91 (m, 12H), 1.05 (br, 40H), 1.33 (br, 26H), 1.55 (br, 8H), 2.02 (br, 8H), 2.50 (br, 8H), 6.90–7.14 (m, 24H), 7.50–7.82 (m, 30H), 7.93–8.08 (m, 10H). <sup>13</sup>C NMR (125 MHz, CDCl<sub>3</sub>): δ 13.96, 14.00, 14.03, 22.4, 22.5, 23.9, 29.2, 30.0, 31.1, 31.66, 31.69, 33.6, 35.0, 35.1, 40.2, 55.2, 55.3, 64.7, 65.8, 120.1, 120.3, 120.9, 121.0, 121.3, 121.5, 121.8, 122.9, 124.55, 124.63, 126.1, 126.2, 126.7, 127.3, 127.4, 127.6, 128.8, 128.9, 129.1, 137.5, 138.5, 139.0, 140.2, 141.0, 141.8, 145.3, 146.7, 149.2, 150.8, 151.9, 152.8, 155.4, 164.0, 164.7. Anal. Calcd: C, 87.13; H, 7.91; N, 3.55. Found: C, 86.56; H, 7.92; N, 3.41.

**Preparation of PFTO-I.** Following the procedure described for the preparation of **WPFTO-II**, a mixture of monomers **1** (47.3 mg, 53.9 μmol), **2** (55.6 mg, 53.7 μmol), **3** (6.80 × 10<sup>-3</sup> M in toluene, 103 μL, 0.70 μmol), **4** (1.09 × 10<sup>-3</sup> M in toluene, 440 μL, 0.48 μmol), and **5** (70.0 mg, 109 μmol) was copolymerized to yield **PFTO-I** (94.9 mg, 73.7%). **PFTO-I** exhibited the same <sup>1</sup>H and <sup>13</sup>C NMR spectroscopic and elemental analysis results as those of **WPFTO-II** because both of these copolymers had very similar chemical structures and compositions.

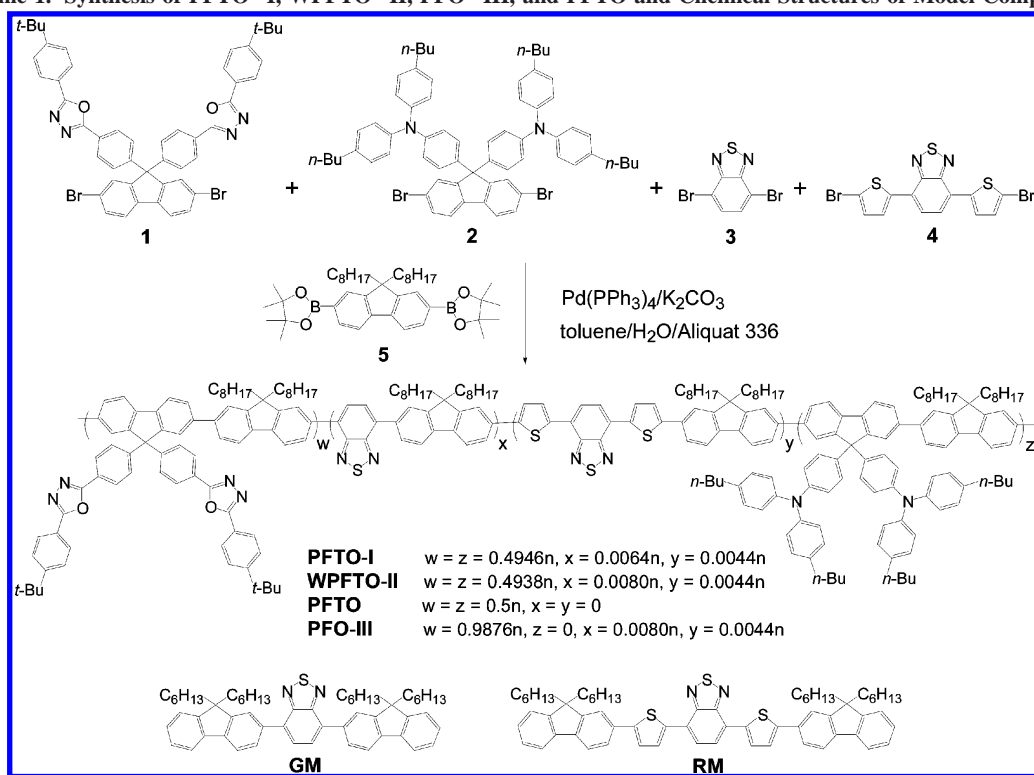
**Preparation of PFO-III.** Following the procedure described for the preparation of **WPFTO-II**, a mixture of monomers **1** (94.5 mg, 107.8 μmol), **3** (6.80 × 10<sup>-3</sup> M in toluene, 128 μL, 0.87 μmol), **4** (1.09 × 10<sup>-3</sup> M in toluene, 440 μL, 0.48 μmol), and **5** (70.0 mg, 109 μmol) was copolymerized to yield **PFO-III** (88.0 mg, 73.2%). <sup>1</sup>H NMR (300 MHz, CDCl<sub>3</sub>): δ 0.67–0.75 (m, 10H), 1.03 (br, 20H), 1.32 (br, 18H), 1.99 (br, 4H), 7.48–7.51 (m, 12H), 7.69–7.73 (m, 6H), 7.93 (d, *J* = 7.8 Hz, 2H), 8.00 (d, *J* = 8.4 Hz, 4H), 8.08 (d, *J* = 7.8 Hz, 4H). <sup>13</sup>C NMR (125 MHz, CDCl<sub>3</sub>): δ 14.0, 22.5, 23.8, 29.1, 29.9, 31.1, 31.6, 35.1, 40.2, 55.3, 65.8, 120.1, 121.0, 121.3, 122.9, 124.5, 126.0, 126.7, 127.3, 127.6, 128.9, 139.0, 139.7, 140.2, 141.8, 149.2, 150.8, 151.8, 155.4, 164.0, 164.7. Anal. Calcd: C, 84.7; H, 7.30; N, 5.07. Found: C, 83.46; H, 7.36; N, 5.07.

## Results and Discussion

**Synthesis of Polyfluorene Copolymers.** Scheme 1 illustrates the synthetic route (and the feed ratio of the comonomers) used to prepare polyfluorene derivatives possessing bipolar pendent groups. The oxidiazole (OXD)-containing monomer **1**, the triphenylamine (TPA)-containing monomer **2**, 4,7-dibromo-2,1,3-benzothiadiazole (**3**), 4,7-bis(5-bromothiophen-2-yl)-2,1,3-benzothiadiazole (**4**), and the diboronate **5** were prepared according to reported procedures.<sup>5a,b,8a,9</sup> The copolymers **PFTO-I** and **WPFTO-II** were synthesized through Suzuki polycondensation using Pd(PPh<sub>3</sub>)<sub>4</sub> as the catalyst and Aliquat 336 as the phase-transfer reagent in a mixture of toluene and aqueous K<sub>2</sub>CO<sub>3</sub> (2.0 M).<sup>13</sup> When polymerization was complete, the end groups of the PF chains were capped by heating the mixture under reflux sequentially with phenylboronic acid and bromobenzene.<sup>14</sup> For the sake of comparison, we also prepared the blue-light-emitting polymer **PFTO** (*M<sub>w</sub>* and *M<sub>n</sub>* were 5.2 × 10<sup>4</sup> and 3.3 × 10<sup>4</sup> g mol<sup>-1</sup>, respectively) through the copolymerization of monomers **1**, **2**, and **5**, as reported previously.<sup>8a</sup>

The dye-attached polyfluorene copolymers are readily soluble in common organic solvents, such as toluene, chlorobenzene, chloroform, and THF. The weight-average molecular weights (*M<sub>w</sub>*) of **PFTO-I** and **WPFTO-II**, as determined through gel permeation chromatography (GPC) using polystyrenes as standards, were 5.8 × 10<sup>4</sup> and 4.7 × 10<sup>4</sup> g mol<sup>-1</sup>, respectively,

Scheme 1. Synthesis of PFTO-I, WPFTO-II, PFO-III, and PFTO and Chemical Structures of Model Compounds



with polydispersities of 2.0 and 2.1, respectively. We investigated these materials' thermal properties using thermogravimetric analysis (TGA) and differential scanning calorimetry (DSC) under a nitrogen atmosphere. As revealed in Figure 1, **PFTO-I** and **WPFTO-II** exhibited their 5% weight losses at temperatures of 425 and 415 °C, respectively, and distinct glass transition temperatures ( $T_g$ ) at 187 and 188 °C, respectively. The relatively high values of  $T_g$  may help to suppress morphological changes from occurring upon exposure to heat, an essential characteristic of polymers intended for use as emissive materials in light-emitting applications.<sup>15</sup>

**Optical Properties.** Figure 2 presents the absorption and emission spectra of **PFTO-I** and **WPFTO-II** in diluted  $\text{CHCl}_3$  solutions and in the solid state. The absorption spectra of **PFTO-I** and **WPFTO-II** are similar to those of **PFTO**, both in solution and in the solid state, with the absorption contributions from the benzothiadiazole (BT) and 4,7-di-(thiophen-2-yl)-benzothiadiazole (DTBT) based units being barely observable in the absorption spectra because of these components' very small abundances in the copolymers. For the same reason,

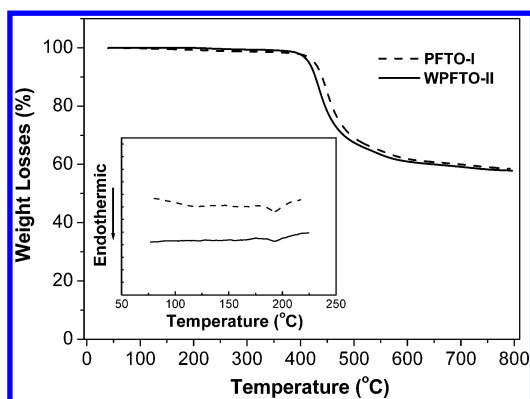


**Figure 1.** TGA thermograms of **PFTO-I** and **WPFTO-II** recorded at a heating rate of 20 °C min<sup>-1</sup>. Inset: DSC traces of **PFTO-I** and **WPFTO-II** recorded at a heating rate of 20 °C min<sup>-1</sup>.

the photoluminescence (PL) spectra of **PFTO-I** and **WPFTO-II** in dilute  $\text{CHCl}_3$  solutions (Figure 2a) are similar to that of **PFTO**. The presence of the BT- and DTBT-based moieties, however, clearly affects the luminescence properties of the thin films. As indicated in Figure 2b, the PL spectra of **PFTO-I** and **WPFTO-II** films spin-coated onto quartz substrates contain, in addition to their PF emissions, two distinct emission bands centered at 520 and 610 nm, which we attribute as originating from the BT- and DTBT-based moieties, respectively. To further understand the interactions between the fluorene segments and the low-energy-emitting species, we prepared two model compounds, **GM** and **RM**, to investigate the optical behavior of the dye-attached moieties in the backbones of the copolymers. Figure 3 displays the optical properties of **GM** and **RM** in dilute  $\text{CHCl}_3$  solutions and the emission spectrum of **PFTO** in the solid state. The absorption spectra of **GM** and **RM** overlap well with the emission spectrum of **PFTO**, which might imply that the efficient energy transfer occurred

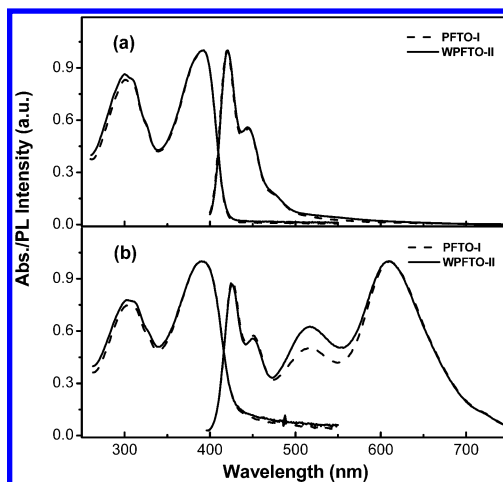


**Figure 2.** Absorption and PL spectra of **PFTO-I** and **WPFTO-II** in (a) dilute  $\text{CHCl}_3$  solutions and (b) the solid state.

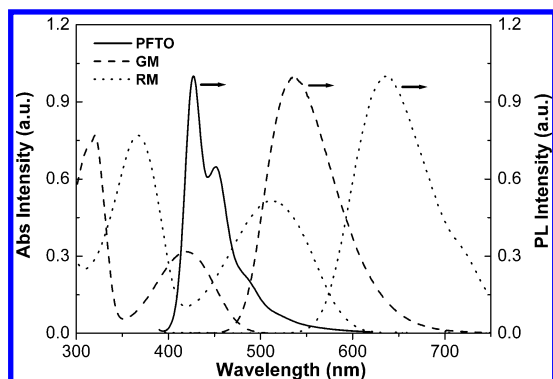


**Figure 3.** PL spectrum of **PFTO** in the solid state and the PL and absorption spectra of **GM** and **RM** in dilute  $\text{CHCl}_3$  solutions.

from the fluorene segments to the low-energy-emitting moieties in the dye-attached copolymers. The enhanced green and red emission intensities in the solid-state PL spectra presented in Figure 2b indicate that energy transfer from the fluorene segments to the low-energy-emitting segments was facilitated through both intra- and interchain channels. On the other hand, the emission of **GM** also overlaps with the absorption of **RM**, which implies that a cascade energy transfer, mediated by BT-based units, could occur from the fluorene segments to the DTBT-based moieties. Because the energy transfer efficiency is very sensitive to the distance between the donor and acceptor, however, such a cascade energy transfer can be discounted because the concentrations of the BT- and DTBT-based units in the dye-attached copolymers were very low; i.e., the average distance between these two moieties was quite long.<sup>8b</sup> In comparison with the intensity of the signal in the PL spectrum of **WPFTO-II**, the green emission of **PFTO-I** had decreased slightly, which is consistent with the small reduction of the feed ratio of monomer **3** in the latter system.

**Electrochemical Properties.** Cyclic voltametry (CV) was employed to investigate the redox behavior of the copolymers and to estimate their HOMO and LUMO energy levels. The electrochemical behavior of the polymer film coated on a glassy carbon electrode was studied in an electrolyte of 0.1 M tetrabutylammonium hexafluorophosphate ( $\text{TBAPF}_6$ ) in acetonitrile; ferrocene was used as the internal standard. **PFTO-I** and **WPFTO-II** exhibited the same redox behavior as **PFTO**, with the onset potentials of the oxidation and reduction at 0.45 and  $-2.32$  V, respectively. In addition, we did not observe any electrochemical behavior attributable to the BT and DTBT units in **PFTO-I** and **WPFTO-II** because of their low contents in the polymer backbones. These results indicate that the introduction of a small number of green- and red-emitting moieties did not affect the electrochemical properties of the resulting polymers. Similar phenomena have been observed from studies of other fluorene-based copolymers.<sup>16</sup> On the basis of the onset potentials, we estimated the HOMO and LUMO energy levels of these three copolymers to be  $-5.25$  and  $-2.48$  eV, respectively, in relation to the energy level of the ferrocene reference (4.8 eV below the vacuum level).<sup>17</sup>

**White Electroluminescence From Dye-Attached PF Copolymers.** To investigate the EL characteristics of the **PFTO-I** and **WPFTO-II** copolymers, we fabricated devices having the configuration ITO/PEDOT/polymer emitting layer/TPBI/Mg:Ag/Ag. The TPBI layer was employed as an electron-transporting layer that would also block holes and confine excitons. Both of these copolymers can emit white light under the influence of an electric field. As depicted in Figure 4, the resulting devices exhibited broadband emissions covering the entire visible region,

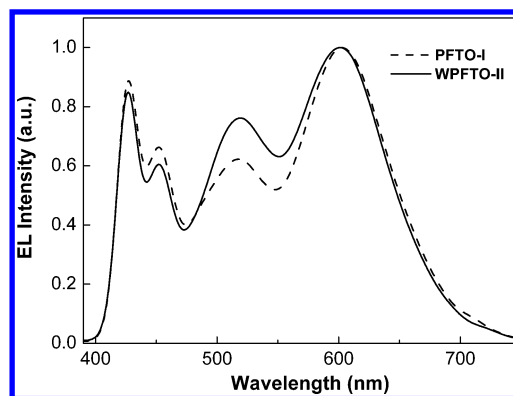


**Figure 4.** EL spectra of the devices incorporating **PFTO-I** or **WPFTO-II** as the emitting layer at an applied potential of 9 V.

from 400 to 700 nm, with main peaks centered at 427, 518, and 602 nm. The peak positions of these three individual bands are quite close to those identified in Figure 3 for the blue-, green-, and red-emitting model compounds. Therefore, we assign the peak in the blue region to the characteristic emission of the polyfluorene moieties and the other two peaks in the green and red regions to the BT- and DTBT-based units, respectively. In addition, we conclude that no exciplex emission contributed to the resulting white electroluminescence because no undesired peaks are visible in the EL spectra. The Commission Internationale d'Éclairage (CIE) chromaticity coordinates of the EL spectral emissions from the **PFTO-I** and **WPFTO-II** devices at a bias of 9 V were (0.37, 0.34) and (0.37, 0.36), respectively, which are both located in the white light region and very close to the equienergy white point (0.33, 0.33). The **PFTO-I**- and **WPFTO-II**-based devices exhibited voltage-independent and stable white light emissions. At lower driving voltage (7 V), the CIE coordinates of the white-emitting devices were (0.36, 0.32) and (0.36, 0.35), respectively; even when the driving voltage increased to 17 V, the CIE color coordinates of these devices changed only slightly, to (0.33, 0.35) and (0.34, 0.38), respectively, but remained in the white light region.

Because the EL spectra of **PFTO-I** and **WPFTO-II** are quite similar to their corresponding PL spectra presented in Figure 2, energy transfer from the fluorene segments to the BT- and DTBT-based units is probably the main operating mechanism involved in the EL process.<sup>18</sup> To better understand the operating mechanism behind the emissions of white light, we employed the model compounds **GM** and **RM** to evaluate the highest occupied molecular orbital (HOMO) and lowest unoccupied molecular orbital (LUMO) energy levels of the green- and red-emitting species embedded in the polymer backbones. Here, the HOMO energy levels of **GM** and **RM** were  $-5.6$  and  $-5.5$  eV, respectively; we determined these values directly using photoelectron spectroscopy.<sup>10</sup> From the absorption onset wavelength of thin film samples, we determined that the optical band gaps of **GM** and **RM** were 2.5 and 2.0 eV, respectively, and calculated the LUMO energy levels from these optical band gaps, assuming a HOMO–LUMO separation equal to the photon energy at the onset of the optical absorption. Figure 5 presents an energy level diagram based on the two model compounds and **PFTO** that we constructed to obtain information regarding the charge-transporting mechanism in the EL devices. The HOMO and LUMO levels of **PFTO** were  $-5.3$  and  $-2.5$  eV, respectively. In this device configuration, holes would be the majority carriers because of the relatively lower injection barrier (0.1 eV) from the ITO/PEDOT electrode to the next organic layer (**PFTO**). According to this energy diagram, it is not possible for the BT- and DTBT-based units to play any

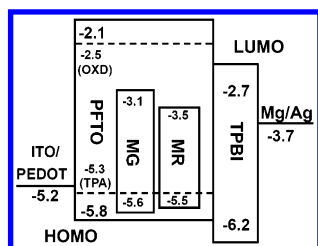


**Figure 5.** Energy level scheme proposed for the devices having the configuration ITO/PEDOT/polymer/TPBI/Mg:Ag.

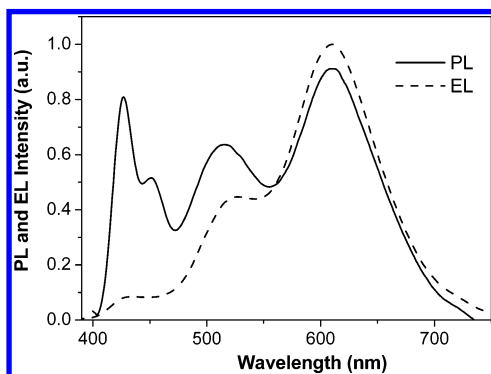


**Figure 6.** PL and EL spectra of the PFO-III film.

roles in the trapping of the major carrier; this finding is consistent with our previous observation of only slight differences between the EL and PL spectra of the individual polymers.<sup>18</sup> To further verify this speculation, we prepared another polyfluorene copolymer (**PFO-III**, Scheme 1,  $M_w$  and  $M_n$  were  $4.0 \times 10^4$  and  $2.2 \times 10^4$  g mol<sup>-1</sup>, respectively), which has a HOMO energy level of  $-5.8$  eV, by replacing the TPA pendent groups of **WPFTO-II** with OXD groups;<sup>9b</sup> in this case, the BT- and DTBT-based units would serve as trapping sites for holes with a depth of 0.2–0.3 eV. Figure 6 displays the EL and PL spectra of the OXD-based PF copolymer. The PL spectrum of **PFO-III** is almost identical to that of **WPFTO-II** in Figure 2b because these copolymers have the same compositions of BT and DTBT units in their backbones. However, unlike **WPFTO-II**, which exhibits similar EL and PL spectra, for **PFO-III** there is a dramatic difference between the EL and PL spectra; the relative intensities of the green and red emissions in comparison with the blue emission are significantly enhanced in the emission spectrum under the influence of an electric field. This result is consistent with the notion that the BT and DTBT units do indeed serve as effective sites for charge trapping in **PFO-III** and that the charge trapping mechanism is significant in the **PFO-III**-based device.<sup>8c,18a</sup>

Figure 7 displays the current density–voltage–luminance ( $I$ – $V$ – $L$ ) curves of the white-light-emitting devices. The **PFTO-I** and **WPFTO-II** devices were turned on at applied voltages of 7.2 and 5.5 (corresponding to 1 cd/m<sup>2</sup>), respectively, and a brightness of 10<sup>3</sup> cd/m<sup>2</sup> was achieved at ca. 10 V for the both devices. As plotted in Figure 8, the maximum luminance efficiency of white electroluminescence was 4.87 cd/A, corresponding to an external quantum efficiency of 2.22%, obtained from the **WPFTO-II** device at a bias of 7 V and a brightness of 59 cd/m<sup>2</sup>. The **PFTO-I** device exhibited a slightly lower luminance efficiency of 3.99 cd/A, which is partially due to its lower contribution from the green emission region, where human eyes are most sensitive among the RGB regions. Table 1 summarizes the characteristics of the white-light-emitting devices incorporating the dye-attached copolymers. At a bias of 10 V, the **WPFTO-II** device reached a brightness of 1146

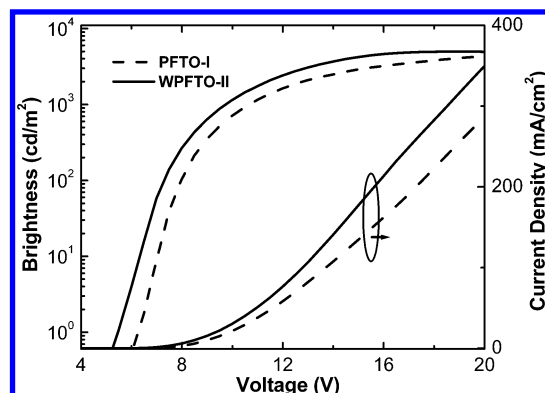


**Figure 7.** Current density–voltage–luminance characteristics of PLEDs incorporating **PFTO-I** and **WPFTO-II**.

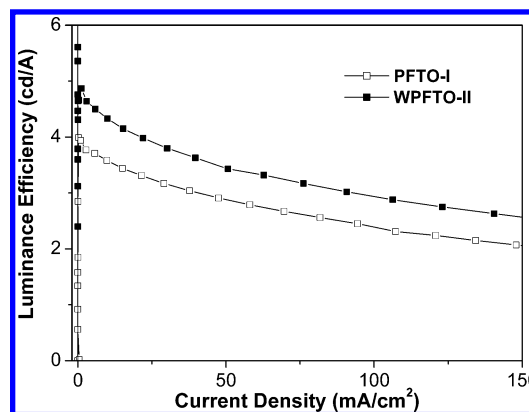


**Figure 8.** Plots of the luminance efficiency as a function of the current density for the white-light-emitting devices.

**Table 1.** Molecular Weights and Electroluminescent Performances of **PFTO-I** and **WPFTO-II** Copolymers

	PFTO-I	WPFTO-II
$M_w, M_n$ ( $10^4$ g mol <sup>-1</sup> )	5.8, 3.0	4.7, 2.3
turn-on voltage (V) <sup>a</sup>	7.2	5.5
voltage (V) <sup>b</sup>	9.9 (13.7) <sup>c</sup>	9.3 (12.8) <sup>c</sup>
brightness (cd/m <sup>2</sup> ) <sup>b</sup>	666 (2390) <sup>c</sup>	804 (2940) <sup>c</sup>
luminance efficiency (cd/A) <sup>b</sup>	3.34 (2.39) <sup>c</sup>	4.03 (2.94) <sup>c</sup>
external quantum efficiency (%) <sup>b</sup>	1.63 (1.17) <sup>c</sup>	1.84 (1.34) <sup>c</sup>
maximum brightness (cd/m <sup>2</sup> )	4320 (at 20 V)	5000 (at 19 V)
maximum luminance efficiency (cd/A)	3.99	4.87
maximum external quantum efficiency (%)	1.95	2.22
EL peak positions (nm) <sup>d</sup>	427, 452, 517, 603	427, 452, 519, 601
CIE coordinates, <sup>d</sup> x and y	0.37 and 0.34	0.37 and 0.36

<sup>a</sup> At 1 cd/m<sup>2</sup>. <sup>b</sup> At 20 mA/cm<sup>2</sup>. <sup>c</sup> Data in parentheses were recorded at 100 mA/cm<sup>2</sup>. <sup>d</sup> At 9 V.

cd/m<sup>2</sup> while retaining a high luminance efficiency of 3.8 cd/A. We note that the EL efficiency of the **WPFTO-II** device is likely to be the highest obtained among fluorescent white-light-emitting devices based on a single-component polymer with the emission contributed from the three primary colors.<sup>7c–e</sup> We attribute this high performance to the balanced charge injection and transport provided by the polar side chains of the dye-attached copolymers as well as to effective exciton confinement within the emitting layer caused by the presence of hole/exciton blocking (TPBI) layer.

## Conclusions

We have demonstrated efficient white electroluminescence from PF-based copolymers (**PFTO-I** and **WPFTO-II**) containing both hole- and electron-transporting pendent groups, with small concentrations of BT-based green-light-emitting and DTBT-based red-light-emitting units covalently linked to the backbone of a bipolar blue-light-emitting polyfluorene, **PFTO**. As a result of partial energy transfer from the blue-fluorescent polyfluorene to the green- and red-fluorescent components, the copolymers exhibit white light emission comprising the individual emissions from the three emissive species. The EL devices based on **PFTO-I** and **WPFTO-II** were turned on at low applied voltages in the region 5–7 V. The luminance efficiency reached as high as 4.87 cd/A, corresponding to an external quantum efficiency of 2.22%. The resulting white electroluminescence exhibited emission contributions from all three primary colors, with the CIE coordinates close to the equal-energy white point. At a brightness of  $10^3$  cd/m<sup>2</sup>, the luminance efficiency could be retained at a high level (ca. 4 cd/A) for the **WPFTO-II** device.

**Acknowledgment.** We thank the National Science Council for financial support. Our special thanks go to Professor C.-H. Cheng for his support during the preparation and characterization of the light-emitting devices.

## References and Notes

- (1) (a) Kido, J.; Kimura, M.; Nagai, K. *Science* **1995**, *267*, 1332. (b) Tasch, S.; List, E. J. W.; Ekström, O.; Graupner, W.; Leising, G.; Schlichting, P.; Rohr, U.; Geerts, Y.; Scherf, U.; Müllen, K. *Appl. Phys. Lett.* **1997**, *71*, 2883.
- (2) Friend, R. H.; Gymer, R. W.; Holmes, A. B.; Burroughes, J. H.; Marks, R. N.; Taliani, C.; Bradley, D. D. C.; Dos Santos, D. A.; Brédas, J. L.; Lögdlund, M.; Salaneck, W. R. *Nature* **1999**, *397*, 121.
- (3) (a) Morgado, J.; Cacialli, F.; Friend, R. H.; Iqbal, R.; Yahioglu, G.; Milgrom, L. R.; Moratti, S. C.; Holmes, A. B. *Chem. Phys. Lett.* **2000**, *325*, 552. (b) Ego, C.; Marsitzky, D.; Becker, S.; Zhang, J.; Grimdale, A. C.; Müllen, K.; MacKenzie, D.; Silva, C.; Friend, R. H. *J. Am. Chem. Soc.* **2003**, *125*, 437. (c) Müller, C. D.; Falcou, A.; Reckefuss, N.; Rojahn, M.; Wiederhorn, V.; Rudati, P.; Frohne, H.; Nuyken, O.; Becker, H.; Meerholz, K. *Nature* **2003**, *421*, 829.
- (4) (a) Pei, Q.; Yang, Y. *J. Am. Chem. Soc.* **1996**, *118*, 7416. (b) Leclerc, M. *J. Polym. Sci., Part A: Polym. Chem.* **2001**, *39*, 2867. (c) Neher, D. *Macromol. Rapid Commun.* **2001**, *22*, 1365. (d) Becker, S.; Ego, C.; Grimdale, A. C.; List, E. J. W.; Marsitzky, D.; Pogantsch, A.; Setayesh, S.; Leising, G.; Müllen, K. *Synth. Met.* **2002**, *125*, 73.
- (5) (a) Herguch, P.; Jiang, X.-Z.; Liu, M. S.; Jen, A. K.-Y. *Macromolecules* **2002**, *35*, 6094. (b) Hou, Q.; Xu, Y.; Yang, W.; Yuan, M.; Peng, J.; Cao, Y. *J. Mater. Chem.* **2002**, *12*, 2887. (c) Yang, R.; Tian, R.; Yan, J.; Zhang, Y.; Yang, J.; Hou, Q.; Yang, W.; Zhang, C.; Cao, Y. *Macromolecules* **2005**, *38*, 244. (d) Su, H.-J.; Wu, F.-I.; Tseng, Y.-H.; Shu, C.-F. *Adv. Funct. Mater.* **2005**, *15*, 1209. (e) Peng, Q.; Kang, E. T.; Neoh, K. G.; Xiao, D.; Zou, D. *J. Mater. Chem.* **2006**, *16*, 376.
- (6) (a) Chen, X. W.; Liao, J. L.; Liang, Y. M.; Ahmed, M. O.; Tseng, H. E.; Chen, S. A. *J. Am. Chem. Soc.* **2003**, *125*, 636. (b) Sandee, A. J.; Williams, C. K.; Evans, N. R.; Davies, J. E.; Boothby, C. E.; Kohler, A.; Friend, R. H.; Holmes, A. B. *J. Am. Chem. Soc.* **2004**, *126*, 7041. (c) Su, H.-J.; Wu, F.-I.; Shu, C.-F.; Tung, Y.-L.; Chi, Y.; Lee, G.-H. *J. Polym. Sci., Part A: Polym. Chem.* **2005**, *43*, 859. (d) Zhen, H.; Luo, C.; Yang, W.; Song, W.; Du, B.; Jiang, J.; Jiang, C.; Zhang, Y.; Cao, Y. *Macromolecules* **2006**, *39*, 1693.
- (7) (a) Buchhauser, D.; Scheffel, M.; Rogler, W.; Tschamber, C.; Heuser, K.; Hunze, A.; Gieres, G.; Henseler, D.; Jakowetz, W.; Diekmann, K.; Winnacker, A.; Becker, H.; Büsing, A.; Falcou, A.; Rau, L.; Vögele, S.; Götting, S. *Proc. SPIE-Int. Soc. Opt. Eng.* **2004**, *5519*, 70. (b) Tu, G.; Zhou, Q.; Cheng, Y.; Wang, L.; Ma, D.; Jing, X.; Wang, F. *Appl. Phys. Lett.* **2004**, *85*, 2172. (c) Liu, J.; Zhou, Q.; Cheng, Y.; Geng, Y.; Wang, L.; Ma, D.; Jing, X.; Wang, F. *Adv. Mater.* **2005**, *17*, 2974. (d) Lee, S. K.; Hwang, D.-H.; Jung, B.-J.; Cho, N. S.; Lee, J.; Lee, J.-D.; Shim, H.-K. *Adv. Funct. Mater.* **2005**, *15*, 1647. (e) Wu, W.-C.; Lee, W.-Y.; Chen, W.-C. *Macromol. Chem. Phys.* **2006**, *207*, 1131.
- (8) (a) Shu, C.-F.; Dodda, R.; Wu, F.-I.; Liu, M. S.; Jen, A. K.-Y. *Macromolecules* **2003**, *36*, 6698. (b) Kim, J. H.; Herguth, P.; Kang, M.-S.; Jen, A. K.-J.; Tseng, Y.-H.; Shu, C.-F. *Appl. Phys. Lett.* **2004**, *85*, 1116. (c) Wu, F.-I.; Shih, P.-I.; Tseng, Y.-H.; Chen, G.-Y.; Chien, C.-H.; Shu, C.-F.; Tung, Y.-L.; Chi, Y.; Jen, A. K.-Y. *J. Phys. Chem. B* **2005**, *109*, 14000.
- (9) (a) Ranger, M.; Rondeau, D.; Leclerc, M. *Macromolecules* **1997**, *30*, 7686. (b) Wu, F.-I.; Reddy, D. S.; Shu, C.-F.; Liu, M. S.; Jen, A. K.-Y. *Chem. Mater.* **2003**, *15*, 269.
- (10) Jung, B.-J.; Lee, J.-I.; Chu, H. Y.; Do, L.-M.; Shim, H.-K. *Macromolecules* **2002**, *35*, 2282.
- (11) Culligan, S. W.; Geng, Y.; Chen, S. H.; Klubek, K.; Vaeth, K. M.; Tang, C. W. *Adv. Mater.* **2003**, *15*, 1176.
- (12) Koizumi, Y.; Seki, S.; Acharya, A.; Saeki, A.; Tagawa, S. *Chem. Lett.* **2004**, *33*, 1290.
- (13) Miyaura, N.; Suzuki, A. *Chem. Rev.* **1995**, *95*, 2457.
- (14) (a) Inbasekaran, M.; Wu, W.; Woo, E. P. U.S. Patent 5,777,070, 1998. (b) Yang, X. H.; Yang, W.; Yuan, M.; Hou, Q.; Huang, J.; Zeng, X. R.; Cao, Y. *Synth. Met.* **2003**, *135*, 189.
- (15) Tokito, S.; Tanaka, H.; Noda, K.; Okada, A.; Taga, Y. *Appl. Phys. Lett.* **1997**, *70*, 1929.
- (16) (a) Liu, J.; Zhou, Q.; Cheng, Y.; Geng, Y.; Wang, L.; Ma, D.; Jing, X.; Wang, F. *Adv. Funct. Mater.* **2006**, *16*, 957. (b) Shih, P.-I.; Tseng, Y.-H.; Wu, F.-I.; Dixit, A. K.; Shu, C.-F. *Adv. Funct. Mater.* **2006**, *16*, 1582.
- (17) Pommerehne, J.; Vestweber, H.; Guss, W.; Mahrt, R. F.; Bäessler, H.; Porsch, M.; Daub, J. *Adv. Mater.* **1995**, *7*, 551.
- (18) (a) Uchida, M.; Adachi, C.; Koyama, T.; Taniguchi, Y. *J. Appl. Phys.* **1999**, *86*, 1680. (b) Virgili, T.; Lidzey, D. C.; Bradley, D. D. C. *Synth. Met.* **2000**, *111*, 203.

MA062192+